Light-Induced Nanosecond Relaxation Dynamics of Rhenium-Labelled Pseudomonas Aeruginosa Azurins

Journal:	*The Journal of Physical Chemistry*
Manuscript ID	jp-2019-108023.R1
Manuscript Type:	Article
Date Submitted by the Author:	n/a
Complete List of Authors:	Pospisil, Petr; J. Heyrovsky Institute of Physical Chemistry, Sykora, Jan; J. Heyrovský Institute of Physical Chemistry of the CAS, v. v. i., Biophysical Chemistry Takematsu, Kana; Bowdoin College Department of Chemistry, Hof, Martin; Ustav fyzikalni chemie J Heyrovskeho Akademie Ved Ceske Republiky, Institute of Phy. Chem. Gray, Harry; California Institute of Technology, Division of Chemistry and Chemical Engineering Vlcek, Antonin; Queen Mary University of London, SBCS

Light-Induced Nanosecond Relaxation Dynamics of Rhenium-Labelled *Pseudomonas aeruginosa* Azurins

Petr Pospíšil,[a] Jan Sýkora,[a] Kana Takematsu,[b] Martin Hof,[a] Harry B. Gray,*[,c] Antonín Vlček*[,a,d]

[a] J. Heyrovský Institute of Physical Chemistry, Czech Academy of Sciences, Dolejškova 3, CZ-182 23 Prague, Czech Republic
[b] Department of Chemistry, Bowdoin College, Brunswick, ME 04011, USA
[c] Beckman Institute, California Institute of Technology, Pasadena, CA 91125, USA
[d] Queen Mary University of London, School of Biological and Chemical Sciences, Mile End Road, London E1 4NS, United Kingdom

Abstract

Time-resolved phosphorescence spectra of $Re(CO)_3(dmp)^+$ and $Re(CO)_3(phen)^+$ chromophores (dmp = 4,7-dimethyl-1,10-phenanthroline, phen = 1,10-phenanthroline) bound to surface histidines (H83, H124, H126) of *Pseudomonas aeruginosa* azurin mutants exhibit dynamic band maxima shifts to lower wavenumbers following 3-exponential kinetics with 1-5 and 20-100 ns major phases, and a 1.1-2.5 μs minor (5-16%) phase. Observation of slow relaxation components was made possible by using an organometallic Re chromophore as a probe whose long phosphorescence lifetime extends the observation window up to ~3 μs. Integrated emission-band areas also decay with 2- or 3-exponential kinetics; the faster decay phase(s) are relaxation-related, whereas the slowest one (360-680 ns (dmp); 90-140 ns (phen)) arises mainly from population decay. As a result of shifting bands, the emission intensity decay kinetics depend on the detection wavelength. Detailed kinetics analyses and comparisons with band-shift dynamics are needed to disentangle relaxation and population decay kinetics if they occur on comparable timescales. The dynamic phosphorescence Stokes shift in Re-azurins is caused by relaxation motions of the solvent, the protein and solvated amino acid side chains at the Re

binding site in response to chromophore electronic excitation. Comparing relaxation and decay kinetics of **Re(dmp)124K122Cu^{II}** and **Re(dmp)124W122Cu^{II}** suggests that ET and relaxation motions in the W122 mutant are coupled. It follows that nanosecond and faster photoinduced ET steps in azurins (and, likely other redox proteins) occur from unrelaxed systems; importantly, these reactions can be driven (or hindered) by structural and solvational dynamics.

Introduction

Optical excitation of photosensitizers covalently appended to proteins can trigger long-range electron-transfer (ET) through the folded polypeptides, eventually oxidizing (or reducing) the natural redox site of the protein. This approach has been widely used to elucidate mechanisms of intraprotein ET[1,2,3] as well as the delivery of electrons or holes to active centers or as a means of protection from oxidative damage.[1,2,4] Understanding these processes could lead to development of "photoenzymes". Efficient charge injection requires the initial ET step to be much faster than the decay of the electronically excited sensitizer to the ground state, hence, (sub)picosecond ET occurs in natural photosynthetic centers (PSI, PSII), flavodoxins, cryptochromes, and photolyases that contain singlet-excited chromophores. On the other hand, the frequently used organometallic photosensitizer $Re(CO)_3(dmp)^+$ (Re(dmp); dmp = 4,7-dimethyl-1,10-phenanthroline), when appended to a surface histidine, has an inherent (unquenched) lifetime of about 1 μs,[5] limiting the observable ET times to ca. 2 μs and faster. (For example, 800 ns $Cu^I \rightarrow$*Re ET was determined[6] in *Re(phen)83AzurinCu^I; * denotes electronic excitation; phen = 1,10-phenanthroline). Of special interest are systems where a tryptophan (W) residue is located near the Re site, such as in *Pseudomonas aeruginosa* azurin mutants **Re(dmp)124W122Cu^I** [5] and **Re(dmp)126W124W122Cu^I**.[7] (For mutant notation, see the

Figure 1 legend and Methods). In these cases, photoinduced W→*Re ET follows multiexponential kinetics with lifetimes ranging from (sub)picoseconds to nanoseconds;[5,7,8] and it does not matter whether the tryptophan residue is placed in the same protein molecule as the chromophore or in a neighboring molecule in a dimer, as long as it is near the chromophore.[9,10] Similarly, $Re(CO)_3$(phen)-type chromophores have been used for rapid photooxidation of aromatic amino acids in ribonucleotide reductases[11,12] and DNA.[13]

The (sub)picosecond - early nanosecond ET timescale determined in Re-tryptophan azurins coincides with that of solvent and protein relaxation motions that take place in tens of femtoseconds (solvent inertial motions),[14] picoseconds (solvent reorientation),[15,16,17,18] and tens of picoseconds - nanoseconds (motions of solvated amino acid side chains),[15,16,17,19] while global conformational fluctuations occur on a microsecond and slower timescales.[20,21,22,23,24] The actual relaxation rates, which depend on the local structure,[17,18,25,26,27,28] have been correlated with enzymatic activity.[29,30,31] Photoexcitation of chromophore-protein constructs triggers such motions in a chromophore binding site and its vicinity, as the protein polar groups and solvent molecules respond to the sudden change of charge distribution in the chromophore. Resulting structural and solvational protein dynamics are experimentally manifested by a time-dependent Stokes shift of the chromophore luminescence to lower energies[15,16,17,18,27,31,32,33,34,35,36] and, in some cases, also by chromophore IR bands shifting to higher wavenumbers.[25,37,38,39,40] The similarity between the timescales of photoinduced ET and relaxation motions means that ET occurs from a nonequilibrated ensemble of electronically excited sensitizer-protein complexes, alongside its relaxation. Such behavior was found for

photoinduced ET in a photosynthetic reaction center[41] and in flavodoxin;[42] and the ET kinetics were interpreted[41,43] in the framework of the Sumi-Marcus theory.[44]

In the particular case of Re-labelled azurins, absorption of a near-UV photon by the Re(dmp) or Re(phen) chromophore produces a singlet metal-to-ligand charge transfer (^{1}MLCT) excited state[25,45,46] that undergoes ~150 fs conversion[45,47] to a long-lived excited state of mixed ^{3}MLCT / $\pi\pi^*$ intraligand (IL) character.[25,45,46,48,49,50] This process is accompanied by a shift of electron density from $Re(CO)_3$ to dmp (or phen) ligand, which changes the orientation of the chromophore dipole moment and decreases its absolute magnitude.[25,38,51] Time-resolved IR (TRIR) spectra of Re-azurins exhibit a dynamic shift of excited-state ν(CO) bands to higher wavenumbers following 400 nm excitation[25] that follows 3-exponential kinetics (2-6, 10-20, 200-600 ps). Based on 2DIR experiments in dipolar solvents,[51,52] the first two kinetics components are attributable to vibrational relaxation (~3.2 ps in MeCN) and bulk-water solvation, respectively. The longest lifetime, which strongly depends on the position of the surface histidine bearing the Re chromophore, was attributed to relaxation motions that change the orientation of the excited Re chromophore relative to the solvated protein, optimizing their electrostatic interactions.[25] For some mutants, the "slow" IR relaxation time increases with increasing concentration[25] due to aggregation.[53] Moreover, time-dependent Re-luminescence anisotropy exhibits a site- and concentration dependent 100-1300 ps decay attributable to rotation or "wobbling" of the Re chromophore relative to the protein.[25,53] Excited-state ν(CO) IR bands of photo-ET-active Re(dmp)-tryptophan azurins simultaneously decrease in intensity and shift higher due to concomitant (ultra)fast ET and relaxation motions, respectively. Accordingly, we have postulated that photoinduced W$\rightarrow$*Re ET in its initial phases

takes place from thermally unequilibrated configurations.[5,7,8,9,10] Although it was not possible to analyze dynamic IR band shifts of these systems quantitatively, TRIR spectra indicated that they span times from early picoseconds to 2-3 ns.[8,10] In addition, we have observed[10] ~50 ps luminescence decay of **Re(dmp)126W124W122** with an amplitude that decreases with increasing detection wavelength, a strong indication of an underlying relaxation process.[31]

Aiming at slower relaxation phases and their possible effects on ET reactivity, we have measured luminescence decay kinetics of Re-azurins in their Cu^{II} forms (Figure 1) at a series of emission wavelengths and reconstructed their time-dependent luminescence spectra. Most of the dynamic Stokes shifts occur on timescales of units and tens of nanoseconds. In addition, low-amplitude hundreds of nanoseconds and microsecond relaxation components were detected taking advantage of long Re(dmp) excited-state lifetimes (hundreds of ns in Cu^{II} azurins, ~1 μs for Cu^{I} or Zn^{II}). These findings have important implications for analyzing experimental kinetics data and interpreting photoinduced ET mechanisms.

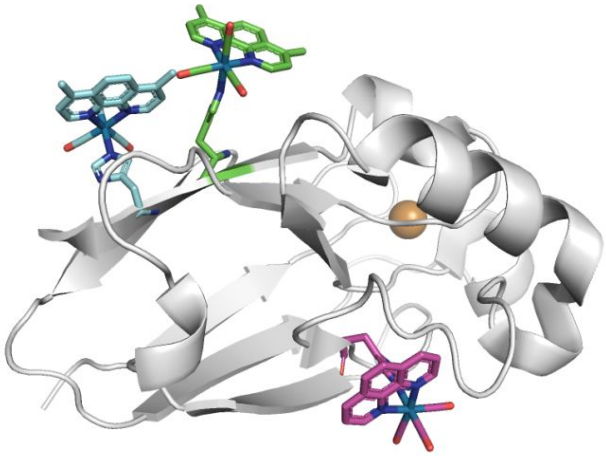

Figure 1. Stylized structure of investigated Re-azurins showing the Re chromophore attached at H124 (green), H126 (blue), and H83 (violet). The Cu atom is shown as a brown sphere. Based on PDBs 2I7O, 6MJS, and 1JZI, respectively.[5,6,25,37]

Methods

Materials. Re-azurins were prepared and labelled at a single surface His residue (H) by reacting azurin mutants with $[Re(H_2O)(CO)_3(phen)]OTf$ or $[Re(H_2O)(CO)_3(dmp)]OTf$ as described previously.[5,6,9,25,53,54,55] The following mutants were used: WT (**83**); W48F/Y72F/Y108F (**83AII Phe**); H83Q/T124H/W48F/Y72F/Y108F (**124K122**); H83Q/T124H/K122W/W48F/Y72F/Y108F (**124W122**); H83Q/T126H/W48F/Y72F/Y108F (**126K122**); and H83Q/T126H/K122F/W48F/Y72F/Y108F (**126F122**). The purity of Re-azurin samples was checked by mass spectrometry. Solutions for luminescence experiments were prepared in 20 mM NaP_i buffer, pH = 7.2. Sample concentrations were kept relatively low (0.15 – 0.5 mM) while sufficient to provide good signals and reasonable data acquisition times.

Spectroscopic and kinetics experiments. Stationary UV-vis absorption and luminescence spectra were recorded on Shimadzu UV2600 and Jobin Yvon (Horiba) FluoroMax-3 spectrometers, respectively. Emission decay kinetics were determined using the time-correlated single photon counting technique (TCSPC) on an IBH 5000 U SPC instrument equipped with a cooled Hamamatsu R3809U-50 microchannel plate photomultiplier with ~40 ps time resolution. Samples were excited at 373 nm with an IBH NanoLED-11 diode laser (80 ps fwhm, 250 kHz repetition rate). The signal was kept below 2% of the light source repetition rate to avoid shortening of the recorded lifetime due to the pile-up effect. To cover the entire emission kinetics, the data were recorded at 10 nm intervals across the luminescence band in a 0-1000 ns range (0.486 ns per channel, ~0.5 ns time resolution). Scattered light was eliminated by 399 nm or 500 nm cut-off filters. Collected decays were fitted using the iterative reconvolution procedure with PicoQuant Fluofit software to a multiexponential function convoluted with the

experimental instrument response function. Time-resolved emission spectra were reconstructed from the fitted decays using a standard procedure and fitted to a log-normal function.[32] Errors of every parameter of fitted decays were calculated as standard deviations by the bootstrap method using FluoFit software (PicoQuant). Then, each position of TRES maxima was calculated using the standard deviation of each parameter of respective decays as upper and lower limits. Errors of TRES maxima positions were estimated within this limit as calculated maximum and minimum values. The error magnitudes are largest for the shortest (extrapolated) times and decrease with increasing time delay. A typical case is shown in Figure S1. To calculate the mean third power of the emission band wavenumber, we have fitted the band areas with 3rd-order polynomial (Matlab spline function) and used eq. 2 of ref.[56]. The integrals were evaluated numerically using 1 cm^{-1} steps. Sample solutions were placed under air in a 1.5 mm fluorescence microcell (Hellma). The temperature was maintained at 21° C; and the sample integrity was checked by repeating the measurement of the decay profile at the first-detected emission wavelength at the end of each experiment.

Results

The structures of the Re-azurins we have studied are shown in Figure 1. A Re(dmp) or Re(phen) chromophore was attached at a histidine in three different positions (H83, H124, H126). These Re-azurins were investigated in air-saturated solutions and in their Cu^{II} forms to avoid artifacts from incomplete degassing and reduction. Each absorption spectrum exhibits a Cys112→Cu^{II} LMCT band at ~630 nm and a Re(dmp) (or Re(phen)) MLCT feature between 350 and 400 nm (Figure 2). Stationary luminescence (emission) occurs at ~562 nm (Re(dmp)) or

~600 nm (Re(phen)), and the emission band overlaps on its red side with the Cu^{II} absorption (Figure 2). Hence, Re luminescence is partly quenched by Förster energy transfer, decreasing the *Re(dmp) lifetime to hundreds of nanoseconds. (Although *Re is thermodynamically able to reduce Cu^{II} in azurins,[54] we have never detected an oxidized Re label by TRIR, ruling out *Re→Cu^{II} oxidative quenching. Similarly, energy transfer is a preferred quenching mechanism for Ru^{II}-polypyridyl chromophores appended to Cu^{II}-azurins.[57])

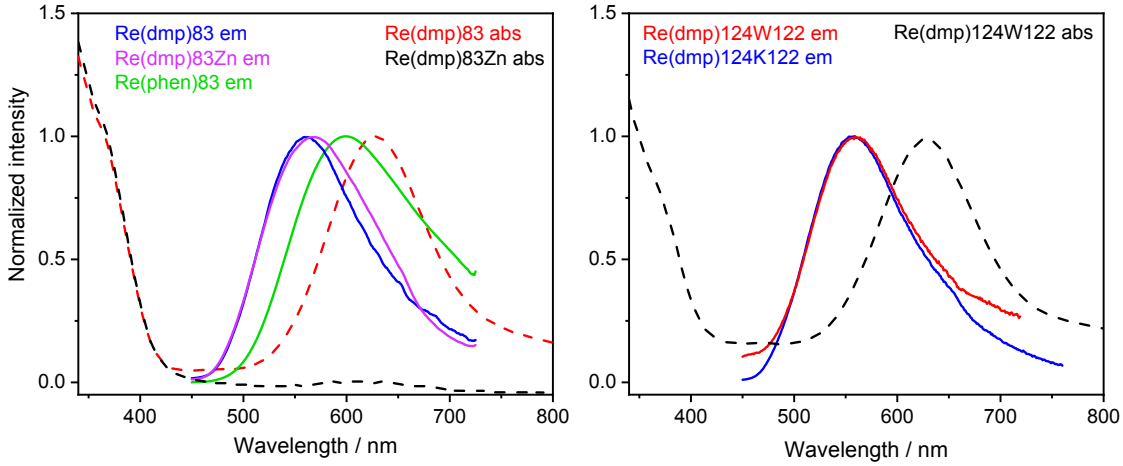

Figure 2. UV-vis absorption and stationary luminescence spectra of Re83 (left) and Re(dmp)124 (right). (Cu^{II} is omitted from the formulas.) These spectra are typical of all investigated species. Emission bands are normalized to 1. (In absolute values, **Re(dmp)124W122** emission is weak, due to ET quenching.)

Time-dependent luminescence spectra were reconstructed from a series of decay profiles measured upon 373 nm excitation with ~0.5 ns time resolution at 10 nm intervals across the luminescence band and fitted to a log-normal line-shape function.[17,32,58] Band maxima of the time-resolved luminescence spectra shift to lower wavenumbers with time (Figures 3, 4), which is a clear indication of dynamic solvent and protein responses to chromophore excitation.[15,16,17,31,32,34,58,59] Most of this dynamic Stokes shift occurs in early tens

of nanoseconds but it continues with a small amplitude into early microseconds (Figure 4). Time-dependences of the band-maximum wavenumbers were fitted to 3-exponential kinetics, producing time constants and amplitudes of the three shift phases, as well as total dynamic shift estimates (500-800 cm^{-1}) and extrapolated peak wavenumbers at time infinity: avg. 17370±50 cm^{-1} (576 nm) and 16380±50 cm^{-1} (610 nm) for Re(dmp) and Re(phen), respectively (Table 1). Since our study focused on "slow" relaxation dynamics, the ~0.5 ns time-resolution did not allow us to capture picosecond relaxation components whose presence was indicated for **Re(dmp)126W124W122**.[10] Hence, the ν_0 and $\Delta\nu$ values reported in Table 1 should be regarded as lower limits.

The band shift is accompanied by 3- or 2-exponential decay of the integrated band area (Figure 3). The first two shift time constants and the faster area decay components are comparable (units- and tens of nanoseconds), both reflecting relaxation kinetics. In contrast, the slowest shift phase, which is solely due to relaxation, is always slower than the slowest area decay component that originates predominantly from population decay. On the other hand, luminescence bandwidths (fwhm) are nearly independent of time, varying randomly in a 5-10% range, comparable with the experimental error.

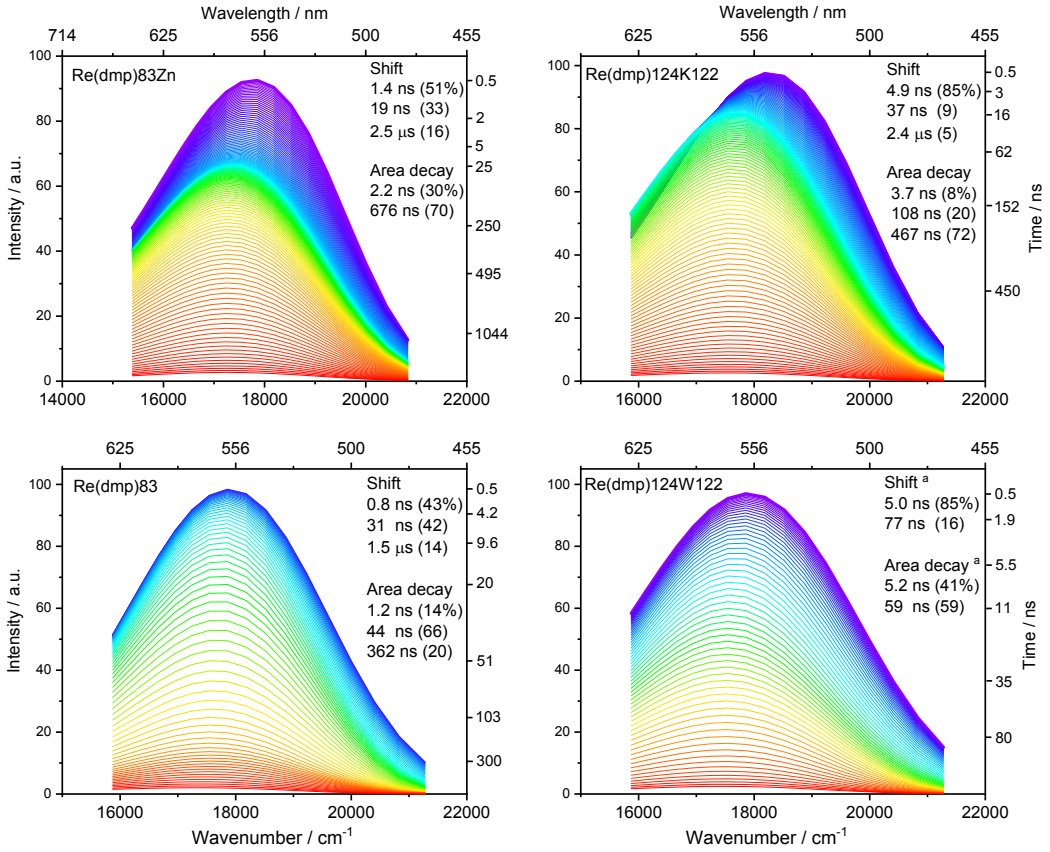

Figure 3. Time-resolved luminescence spectra and kinetics of the dynamic shift and band-area decays of selected Re(dmp)-azurins. Spectral evolution is shown from 0.5 ns (blue) to 2.2 µs (**Re(dmp)83Zn**), 1.1 µs (**Re(dmp)83**), 1.5 µs (**Re(dmp)124K122**), and 250 ns (**Re(dmp)124W122**). Left axes show normalized emission intensity. Left axes indicate the time evolution of the band maxima. [a] Statistically equivalent 3-exponential fits: 2 (12%), 6 (74%), 125 ns (14%) for shift and 4.4 (32%), 11.8 (13%), and 64 ns (56%) for area decay. The spectra shown were obtained by fitting the experimental data with a log-normal function.[32]

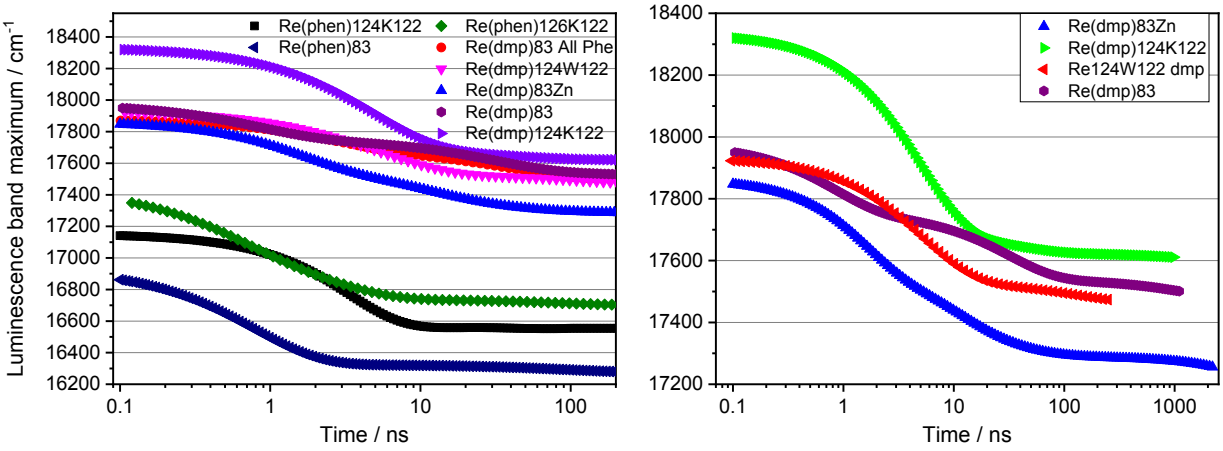

Figure 4. Time-dependence of luminescence band-maximum wavenumbers of Re-azurins. Left: Behavior of all investigated mutants over the first 200 ns. Right: Behavior of selected mutants until the longest experimentally accessible times. (A typical curve including experimental errors is shown in Figure S1.)

Table 1. Kinetics parameters of dynamic shifts of luminescence band maxima of Re-azurins.[a]

	[mM]	A_1 %	A_2 %	A_3 %	τ_1 [ns]	τ_2 [ns]	τ_3 [ns]	ν_0 [cm^{-1}][b]	$\Delta\nu$ [cm^{-1}][c]
Re(dmp)124K122	0.50	85	9	5	4.9	37	2420	18330	780
Re(dmp)124W122	0.15	12	74	14	2.0	6	125	17930	480
Re(dmp)83	0.40	43	42	14	0.8	31	1465	17970	520
Re(dmp)83 All Phe	0.50	45	42	13	2.6	37	>1000	17870	670
Re(dmp)83Zn	0.50	51	33	16	1.4	19	2490	17860	660
Re(phen)83	0.45	92	8	0	0.8	93	-	16900	650
Re(phen)124K122	0.45	100	0	0	3.3	-	-	17150	600
Re(phen)126K122[d]	0.30	49	46	5	0.5	2.4	88	17410	760

[a] Maximal ν_0, ν_∞, and $\Delta\nu$ errors are $\pm$180, $\pm$50, and $\pm$160 cm^{-1}, respectively. τ accuracy is better that $\pm$8%, typically 1-2%. Larger errors occur in some cases for τ_3: $\pm$16% (**Re(dmp)124K122**), $\pm$50% (**Re(dmp)83**), $\pm$24% (**Re(dmp)83Zn**). [b] Maximum wavenumber extrapolated to 0 ps. [c] ν_0-ν_∞ [d] Time-resolved emission spectra of two more Re126 mutants were investigated over a 40 ns range: **Re(dmp)126K122**: ca. 5.8 ns shift, 2.6 and estimated 440 ns area decay; **Re(dmp)126F122**: 4.7 ns shift, ν_0 = 17970 cm^{-1}, $\Delta\nu$ = 662 cm^{-1} and 0.8, 4.0, ca. 440 ns area decay.

Dynamic band shifts cause luminescence intensity decay profiles to change with the detection wavelength from a prominent fast decay at the blue side of the emission bands to an initial rise and slower decay in the red. This behavior is typical[17,18,31,59] for relaxation processes. Re(dmp)- (Figure 5) and Re(phen)-azurins (Figure S2) show qualitatively the same decay profiles, but Re(phen) decays faster. As an alternative means of data analysis, the set of decay profiles measured for each sample at different wavelengths was fitted globally to a triexponential function with linked lifetimes and wavelength-dependent amplitudes that are displayed in Figures 6 and S3. Alternatively to global fitting, decay profiles were fitted

individually, producing different lifetime values at different luminescence wavelengths (Table S1).

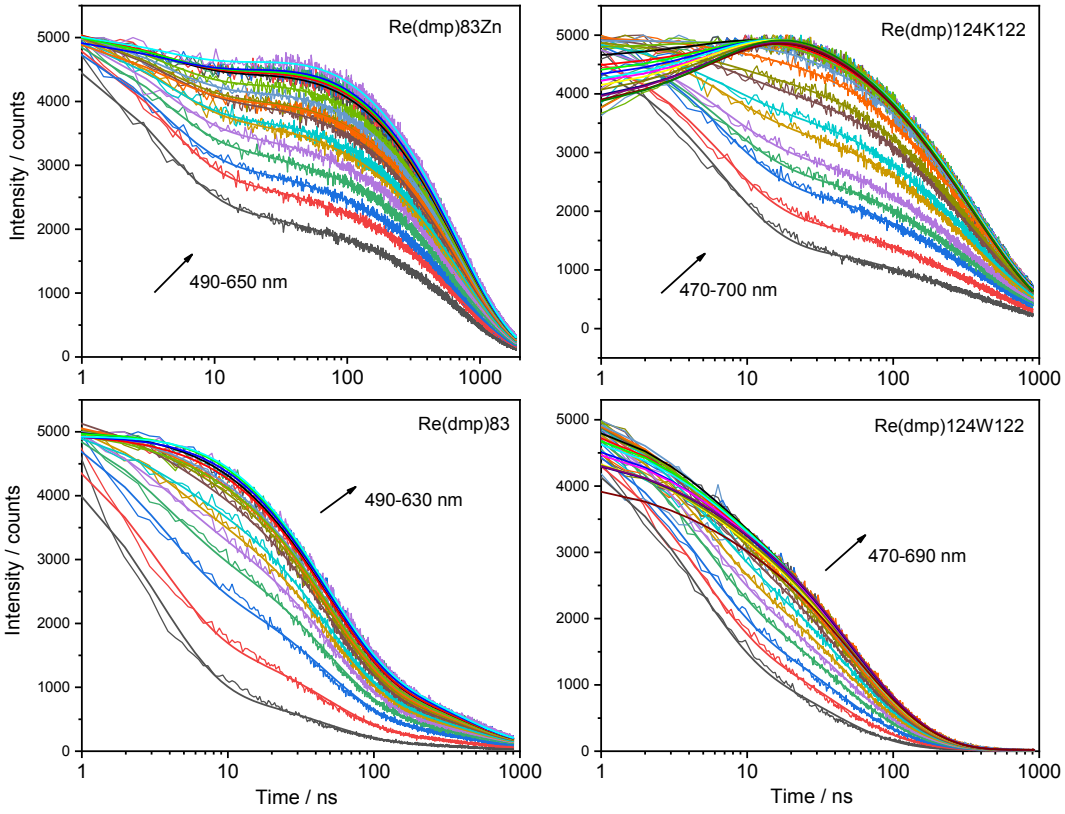

Figure 5. Luminescence decay profiles of selected Re(dmp)-azurins measured at different emission wavelengths in 10 nm intervals. Raw experimental data are shown together with their global fits. Instrument time resolution was limited to ~0.5 ns in order to capture "slow" decay and relaxation kinetics. Data acquisition stopped at 5000 counts. (Decay profiles of Re(phen)-azurins are shown in Figure S2.)

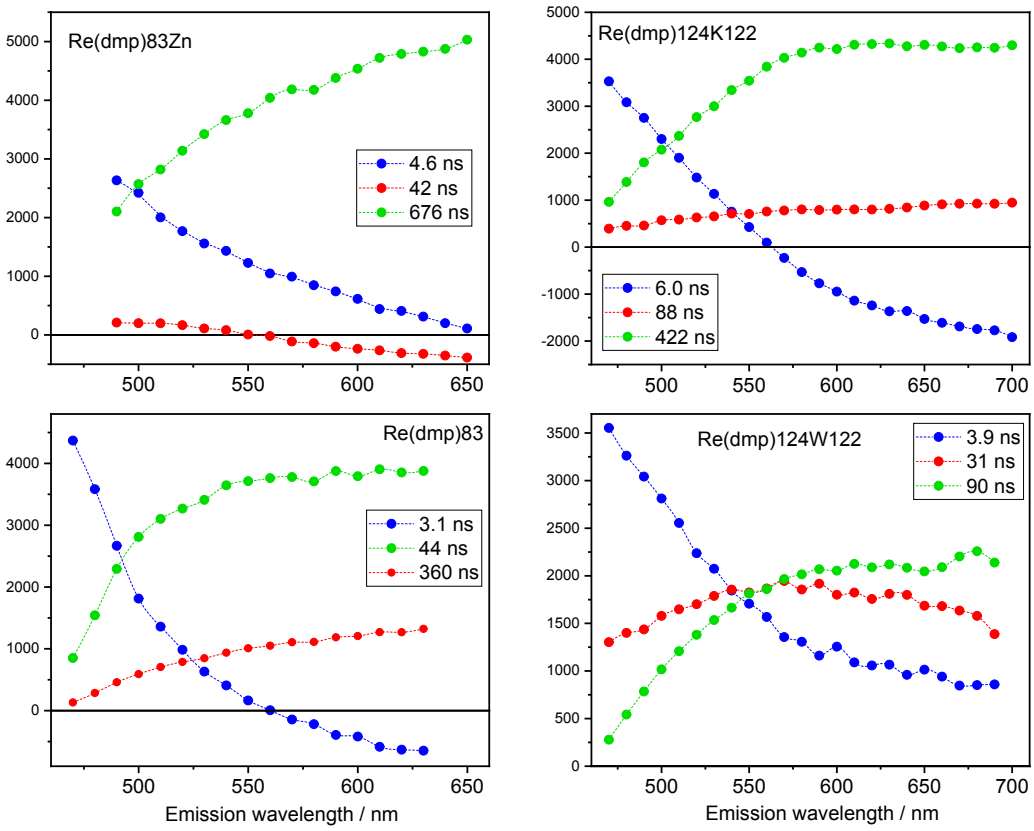

Figure 6. Luminescence decay lifetimes of selected Re(dmp)-azurins and wavelength-dependences of the corresponding amplitudes (i.e., decay associated spectra). Obtained by 3-exponential global fitting of intensity decays shown in Figure 5. (For Re(phen)-azurins, see Figure S3.) Lifetime accuracy ±2% or better. Amplitude accuracy 5% or better, larger errors occur for the blue data (red for Re(dmp)83) at and around switching from positive to negative values, thereby indicating that 2-exponential fits would be sufficient in these regions.

Discussion

Excitation of a Re chromophore at an azurin surface triggers multiscale relaxation motions that span times from picoseconds to early microseconds. Picosecond relaxation phases were monitored by dynamic shifts of excited-state IR bands that, however, abate in 1-3 ns.[8,10,25,37,38] Detecting slow relaxation motions by dynamic Stokes shift requires probes with long-lived excited states whose emission is sensitive to the molecular surroundings. Re chromophores are particularly suitable probes, as their 600-1000 ns phosphorescence lifetimes

allow capturing dynamic shifts up to ca. 3 μs, while their emission energies respond to the changes in the environment. Notably, dynamic phosphorescence shifts have been used only rarely, for example to observe collective polypeptide movements in cyt *c* (with Zn-porphyrin[20]), and dynamics of glass-forming solvents using $Ru(bpy)_2(CN)_2$ as a probe.[33]

The investigated azurin mutants show qualitatively similar relaxation behavior, while actual parameter values depend on the chromophore (Re(dmp) vs. Re(phen)) and the position at the azurin surface. Electronic excitation and ultrafast ISC abruptly change the charge distribution over the Re chromophore, perturbing its interactions with solvent molecules and surrounding amino-acid residues (Figure S4). In addition, energy dissipation during ISC (<<1 ps) and vibrational relaxation (~3 ps)[51,52] could cause local heating. These ultrafast perturbations place the Re binding site far from its energy minimum. Ensuing solvent and protein motions then reorganize local solvation and structure, driving the system toward a new equilibrium configuration with nonbonding electrostatic interactions optimized to the charge distribution in the excited chromophore. Different kinds of motions can be responsible for ns-μs emission shifts, depending on the local binding-site structure (shown in Figure S3). Solvent restructuring, motions of nearby amino acid side chains or the peptide backbone, H-bonding changes, as well as rotation/wobbling of the $Re(CO)_3$(dmp) unit relative to the peptide (evidenced by time-resolved anisotropy)[25,48,53] should be considered. Generally, faster relaxation of Re(phen)- than Re(dmp)-azurins can be attributed to the smaller size of the Re(phen) chromophore. ^{15}N-NMR studies[22,23] have shown that the azurin core is rather rigid (as expected for a β-barrel protein), undergoing only small-amplitude picosecond internal motions, whereas the loops are much more flexible. In **Re(dmp)83Zn** and **Re(dmp)83**, the H83 residue bearing the chromophore is

part of a flexible loop; and the highly flexible D76-D77 loop and K101 side chain lie close (Figure S4). This very flexible environment allows for large-scale restructuring, possibly manifested by the relatively large amplitudes and long τ_2 and τ_3 relaxation times (Table 1). (**Re(dmp)83Zn**, which undergoes neither electron nor energy transfer, exhibits similar relaxation kinetics as **Re(dmp)83**. Shortening of the τ_3 relaxation component from 2.5 to 1.5 μs in **Re(dmp)83** is probably caused by the *Re(dmp) luminescence lifetime shortening by *Re→Cu^{II} energy transfer that shorten the investigated time interval.) Temporal evolution of multiple interactions can operate in the case of **Re(dmp)126K122** and **Re(phen)126K122**: there is a flexible Q107 sidechain whose terminal -$C(O)NH_2$ lies below the phen ligand and its motions will perturb the local electrical field. The T124 –OH group interacts with an equatorial C≡O ligand whose depopulation upon MLCT excitation will diminish H-bonding. Also, the terminal K128 (lying close to the H126 imidazole) was identified[22] as one of the most flexible residues. As the chromophores in **Re(dmp)124K122** and **Re(phen)124K122** are relatively far from the nearest K122 and N18 sidechains, relaxation is likely determined by solvation. Accordingly, the dynamic phosphorescence shift of **Re(phen)124K122** is the fastest of all investigated azurins (3.3 ns), and single-exponential. It is much faster than that of **Re(phen)126K122**, where multiple interactions with amino acid residues likely account for the 3-exponential relaxation dynamics. Like the phen complex, relaxation of **Re(dmp)124K122** is dominated (85%) by a single fast (5 ns) component. The dmp-W122(indole) ππ stacking is the defining interaction in **Re(dmp)124W122**; it likely makes the binding site rather rigid. Accordingly, the total Stokes shift ($\Delta\nu$) is the smallest of all investigated species. Relaxation is relatively fast, probably dominated by solvation, perhaps with a contribution from Q107 sidechain motions.

As NMR studies[22,23,24] have demonstrated that conformational equilibria are established in 100 ms (or slower), they cannot affect the phosphorescence dynamics. Moreover, the populations of alternative conformational states are very low.[24]

Relaxation-induced band shifts are accompanied by integrated area decays (Figure 3) whose faster kinetics components are related to relaxation processes. (A similar observation was made on [Re(Et-pyridine)$(CO)_3$(2,2'-bipyridine)]$^+$ in ionic liquids.[38]) This behavior is in part attributable to a linear decrease of the radiative rate constant with the mean third power of the frequency (or wavenumber) of the emission band ($<\nu^3>$), which decreases with time as the band shifts in the course of relaxation.[56] However, this is not the only reason, since the area decreases during early relaxation phases with decreasing $<\nu^3>$ often nonlinearly and the slopes vary among investigated Re-azurins (Figure 7). It appears[34,60] that the excited-state character changes during relaxation, whereby the $\pi\pi^*$(dmp) intraligand contribution to the emissive excited-state wave function decreases and the MLCT contribution increases with time;[38,45,61,62] and the luminescence quantum yield decreases concomitantly. At early times, **Re(dmp)83Zn** and **Re(dmp)83** exhibit deviations from the expected linear dependence. **Re(dmp)124K122** is close to a linear dependence, possibly because of the high solvent exposure of the Re chromophore that would accelerate excited-state evolution to shorter times (before the investigated range). At longer times, phosphorescence band areas of **Re(dmp)83Zn** and **Re(dmp)124K122** show a sharp drop that is essentially independent of $<\nu^3>$ (marked red in Figure 7); and the corresponding decay lifetimes (676, 467 ns) are much shorter than the slowest relaxation time constant τ_3 (~2.5 μs). In this case, the slowest area decay lifetime can be approximately identified with the population decay lifetime. On the other hand, **Re(dmp)83**

exhibits a fast area decrease after ~10 ns that does not become <ν^3> - independent. This behavior indicates that the relaxation-induced band shift and changing excited-state character occur simultaneously with population decay. Compared with other investigated Re-azurins, the band area of **Re(dmp)124W122** decreases with <ν^3> much faster across the whole time range, owing to a convoluted band shift and multiexponential population decay caused by ET between *Re and W122[5,8] making it impossible to distinguish population decay and relaxation kinetics.

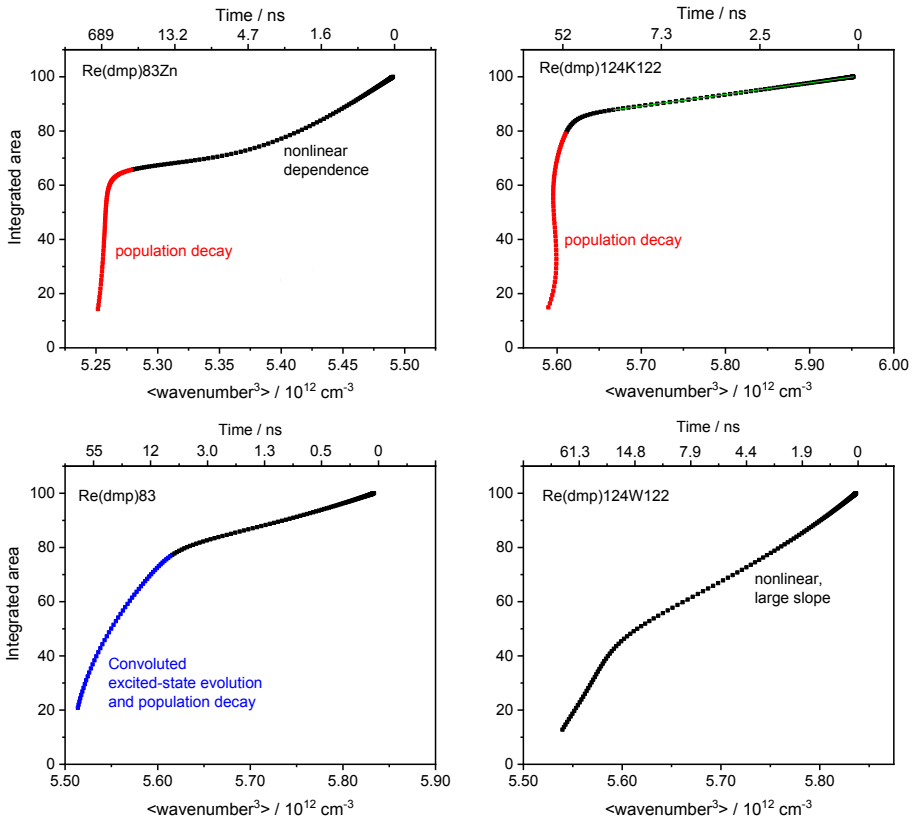

Figure 7. Dependence of integrated emission band areas on mean third power of the emission wavenumber measured for selected Re-azurins. Delay times corresponding to selected area values are shown in the top axes.

Excited-state quenching kinetics and mechanisms are often investigated by measuring emission decay kinetics in a narrow spectral range at or close to the band maximum, neglecting

possible simultaneous band shifts. However, data shown in Figures 5, 6, S2, and S3 demonstrate that relaxation-induced band shifts lead to different emission decay profiles at different wavelengths across emission bands. In such situations, neither global multiexponential fitting of decay profiles measured across the emission band nor single-wavelength decay kinetics can disentangle simultaneous relaxation and population decay kinetics without more detailed data inspection and analysis. Figures 6 and S3 show results of global triexponential fits: lifetimes and corresponding decay associated spectra (DAS). With the exception of **Re(dmp)124W122,** the similarity between the first two decay lifetimes and the τ_1, τ_2 band-shift time constants (Table 1) indicate that the first two decay lifetimes are attributable to relaxation processes. The third (longest) lifetime (that is much shorter than τ_3 and similar to the slowest integrated band area decay lifetime) can be approximately identified with the excited-state population decay to the ground state. Decay associated spectra show changing contributions of individual decay kinetics components across the emission band, visualizing how the fast decay that is predominant on the blue side vanishes or becomes a rise in the red (Figure 6). The longest (population) decay component is most prominent for **Re(dmp)83Zn**, but its relative contribution is diminished in **Re(dmp)83**, owing to energy transfer to Cu^{II}. It also is prominent for **Re(dmp)124K122** , where energy transfer is slower (~1.1 vs. ~0.76 μs) due to a longer Re-Cu distance (17.3 vs. 16.8 Å) and a different chromophore orientation. Re(phen)-azurins exhibit similar behavior to their Re(dmp) counterparts with comparable values of the two relaxation-related decay lifetimes (2-3 and 30-40 ns), whereas the longest decay phase is shorter (Figures S2, S3). An alternative approach, fitting decay profiles at different wavelengths individually, leads to different lifetime values as well as amplitudes at different wavelengths (Table S1). While a 3-exponential function is

required in the blue and red parts of the emission band, 2-exponential fits often are sufficiently close to the maximum, so assigning lifetimes to particular excited-state processes cannot easily be done in the absence of other data. While globally linked lifetimes and corresponding decay associated spectra offer better insights into luminescence dynamics, neither global nor individual decay analysis unequivocally distinguishes between relaxation- and population-related kinetics (and we do not see any physical reason to prefer one way of analysis over the other). Luminescence decay kinetics could lead to erroneous mechanistic conclusions when used to study excited-state reactions that occur on the same timescale as relaxation processes. This is usually no problem for molecular systems in nonpolar or dipolar solvents where relaxation is ultrafast,[32] but ET and relaxation could become convoluted for chromophores in complex media (ionic liquids, polymers and supramolecular systems, biomolecules). In the present case, correct interpretation of the decay kinetics was possible by comparison with band-shift dynamics. Generally, luminescence decay kinetics should be collected over a broad spectral range (or the time evolution of the whole emission band should be followed, e.g. with a streak camera). Importantly, band-shift kinetics should be determined separately and combined with results from time-resolved spectral techniques that are sensitive differently to relaxation processes.

Re(dmp)124W122Cu^{I} presents the most complicated case where relaxation and population decay kinetics are convoluted over the whole investigated temporal range due to (ultra)fast ET from the W122 indole to electronically excited Re(dmp).[5,8] ET steps at different stages of *Re(dmp) relaxation were identified by TRIR spectroscopy, while integrated luminescence measured at wavelengths >450 nm revealed lifetimes of 35 ps (growth), 363 ps

(decay), and 25 ns (decay).[5] Analyzing luminescence, TRIR, and time-resolved visible absorption kinetics data together, it was concluded that, after several ultrafast relaxation and hot-ET steps, an equilibrium is established between the ^{3}MLCT excited state *Re^{II}(dmp$^{\bullet-}$)124W122Cu^{I} and the charge-separated state Re^{I}(dmp$^{\bullet-}$)124(W122$^{\bullet+}$)Cu^{I} with forward- and back time constants of 0.5 and 1.4 ns.[5] TRIR,[5,8,25] as well as the present luminescence experiments (Table 1), show that relaxation of the Re binding site and its environment is slower than or comparable with ET steps. Comparing global luminescence decay fits of **Re(dmp)124K122** and its **W122** counterpart (Figure 6) reveals an interesting behavior of the middle decay component. It shortens from 88 ns (K) to 31 ns (W), and the corresponding DAS changes from a steady rise to the red (K) to a broad peak around the emission band maximum (W) (Figure 6). It follows that the luminescence 31 ns decay kinetics in **Re(dmp)W122** likely is dominated by *Re(dmp) population changes, possibly convoluted with relaxation. This finding agrees with our previous kinetics study that found similar (25 ns) kinetics attributable to the ET equilibrium.[5,8] The third luminescence decay component of 90 ns (~60 ns for area decay) could have a significant relaxation contribution, corresponding to the 125 ns τ_3 shift time constant. On the other hand, the 3.9 ns decay component and the steep increase of its amplitude in the blue part of the emission band are common for all investigated Re-azurins, regardless of their ET photoreactivity[7,8,9,10] (Figures 6 and S3, Table S1); and this behavior can be attributed predominantly to relaxation.

Concluding Remarks

Optical excitation of a Re carbonyl-polypyridine chromophore covalently attached to a histidine residue at the azurin surface triggers relaxation processes of the solvent and the protein in and around the Re binding site that optimize electrostatic interactions with the excited chromophore, as well as its solvation. Relaxation occurs in several phases that span times from picoseconds[10,25] to tens of nanoseconds and persists with low-amplitudes to early microseconds, depending on the chromophore position.

Relaxation is spectroscopically demonstrated by a dynamic shift of the luminescence band to lower energies whose quantitative analysis provides the values of relaxation kinetics parameters. The relaxation-related band shift leads to band-area decay and makes luminescence intensity decay kinetics dependent on the emission wavelength. Great care must be taken to disentangle relaxation and excited-state population changes (decay, ET or EnT reactions, etc.) if they occur on comparable timescales. A correct interpretation then requires measuring decay time profiles across the whole emission band (or determining the band-area decay) and comparing the decay kinetics with separately determined band-shift dynamics.

Re carbonyl-polypyridines[50,63] with long-lived ^{3}MLCT excited states are particularly suitable probes to detect "slow" relaxation processes by dynamic phosphorescence shifts, owing to long excited-state lifetimes and relatively intense and environmentally sensitive photoemissions. In addition to phosphorescence, they are also IR probes, capable of monitoring excited-state relaxation and reactions by time-resolved IR absorption and 2D-IR spectroscopy.[25,38,51,52,64] Also, Re complexes can be incorporated into a broad range of supramolecular environments. Re carbonyl-polypyridines are also strong photooxidants and, in redox proteins or DNA, electronic excitation can trigger relaxation dynamics together with ET.

In the case of Re-tryptophan-azurins, relaxation occurs on the same timescale as excited-state ET that initiates electron (hole) hopping through the protein,[5,7,8] as well as across protein-protein interfaces.[9,10] It is possible that matching ET and relaxation timescales is not coincidental but functional, whereby some of the relaxation movements are coupled with ET. Further experimental work, most especially in combination with relevant theory, likely will shed additional light on these dynamics processes.

■ ASSOCIATED CONTENT

Supporting Information

The Supporting Information is available free of charge on the ACS Publications website at DOI….

Luminescence decay profiles of Re(phen)-azurins and their global fits, results of fits of Re(dmp)-azurin decay kinetics at selected luminescence wavelengths.

■ AUTHOR INFORMATION

Corresponding Authors
*E-mail: hbgray@caltech.edu
*E-mail: avlcek@qmul.ac.uk

ORCID
Kana Takematsu: 0000-0002-2334-336X
Jan Sýkora: 0000-0003-0936-9368
Harry B. Gray: 0000-0002-7937-7876
Martin Hof: 0000-0003-2884-3037
Antonín Vlček: 0000-0002-6413-8311

Notes

The authors declare no competing financial interest

■ ACKNOWLEDGMENTS

This work was supported by the Czech Science Foundation (GAČR) grant 17-011375, the Czech Ministry of Education (MŠMT) grant LTAUSA18026, EPSRC grant (UK) EP/R029687/1, and National Institute of Diabetes and Digestive and Kidney Diseases of the National Institutes of Health under award number R01DK019038. The content is solely the responsibility of the authors and does not necessarily represent the official views of the National Institutes of Health. Yuling Shen (Caltech) is acknowledged for her help with protein preparation.

References

1. Winkler, J. R.; Gray, H. B., Long-Range Electron Tunneling. *J. Am. Chem. Soc.* **2014,** *136*, 2930−2939.
2. Winkler, J. R.; Gray, H. B., Electron Flow through Metalloproteins. *Chem. Rev.* **2014,** *114*, 3369−3380.
3. Gray, H. B.; Winkler, J. R., Long-Range Electron Transfer. *Proc. Natl. Acad. Sci. USA* **2005,** *102*, 3534-3539.
4. Gray, H. B.; Winkler, J. R., The Rise of Radicals in Bioinorganic Chemistry. *Isr. J. Chem.* **2016,** *56*, 640–648
5. Shih, C.; Museth, A. K.; Abrahamsson, M.; Blanco-Rodriguez, A. M.; Di Bilio, A. J.; Sudhamsu, J.; Crane, B. R.; Ronayne, K. L.; Towrie, M.; Vlček, A., Jr.; Richards, J. H.; Winkler, J. R.; Gray, H. B., Tryptophan-Accelerated Electron Flow Through Proteins. *Science* **2008,** *320*, 1760-1762.
6. Crane, B. R.; Di Bilio, A. J.; Winkler, J. R.; Gray, H. B., Electron Transfer in Single Crystals of Pseudomonas aeruginosa Azurins. *J. Am. Chem. Soc.* **2001,** *123*, 11623-11631.
7. Takematsu, K.; Williamson, H. R.; Nikolovski, P.; Kaiser, J. T.; Sheng, Y.; Pospíšil, P.; Towrie, M.; Heyda, J.; Hollas, D.; Záliš, S.; Gray, H. B.; Vlček, A.; Winkler, J. R., Two Tryptophans are Better than One in Accelerating Electron Flow Through a Protein. *ACS Cent. Sci.* **2019,** *5*, 192−200.
8. Blanco-Rodríguez, A. M.; Di Bilio, A. J.; Shih, C.; Museth, A. K.; Clark, I. P.; Towrie, M.; Cannizzo, A.; Sudhamsu, J.; Crane, B. R.; Sýkora, J.; Winkler, J. R.; Gray, H. B.; Záliš, S.; Vlček, A., Jr., Phototriggering Electron Flow through Re^{I}-modified *Pseudomonas aeruginosa* Azurins. *Chem. Eur. J.* **2011,** *17*, 5350 – 5361.
9. Takematsu, K.; Williamson, H.; Blanco-Rodríguez, A. M.; Sokolová, L.; Nikolovski, P.; Kaiser, J. T.; Towrie, M.; Clark, I. P.; Vlček, A., Jr.; Winkler, J. R.; Gray, H. B., Tryptophan-Accelerated Electron Flow Across a Protein-Protein Interface. *J. Am. Chem. Soc.* **2013,** *135*, 15515−15525.
10. Takematsu, K.; Pospíšil, P.; Pižl, M.; Towrie, M.; Heyda, J.; Záliš, S.; Kaiser, J. T.; Winkler, J. R.; Gray, H. B.; Vlček, A., Hole Hopping Across a Protein-Protein Interface. *J. Phys. Chem. B* **2019,** *123*, 1578−1591.
11. Olshansky, L.; Stubbe, J.; Nocera, D. G., Charge-Transfer Dynamics at the α/β Subunit Interface of a Photochemical Ribonucleotide Reductase. *J. Am. Chem. Soc.* **2016,** *138*, 1196−1205.
12. Olshansky, L.; Greene, B. L.; Finkbeiner, C.; Stubbe, J.; Nocera, D. G., Photochemical Generation of a Tryptophan Radical within the Subunit Interface of Ribonucleotide Reductase. *Biochemistry* **2016,** *55*, 3234−3240.
13. Olmon, E. D.; Sontz, P. A.; Blanco-Rodríguez, A. M.; Towrie, M.; Clark, I. P.; Vlček, A., Jr.; Barton, J. K., Charge Photoinjection in Intercalated and Covalently Bound $[Re(CO)_3(dppz)(py)]^+$ - DNA Constructs Monitored by Time-Resolved Visible and Infrared Spectroscopy. *J. Am. Chem. Soc.* **2011,** *133*, 13718–13730.
14. Jumper, C. C.; Arpin, P. C.; Turner, D. B.; McClure, S. D.; Rafiq, S.; Dean, J. C.; Cina, J.; Kovac, P. A.; Mirkovic, T.; Scholes, G. D., Broad-Band Pump−Probe Spectroscopy Quantifies Ultrafast Solvation Dynamics of Proteins and Molecules. *J. Phys. Chem. Lett.* **2016,** *7*, 4722−4731.
15. Nilsson, L.; Halle, B., Molecular Origin of Time-Dependent Fluorescence Shifts in Proteins. *Proc. Natl. Acad. Sci. USA* **2005,** *102*, 13867-13872.
16. Golosov, A. A.; Karplus, M., Probing Polar Solvation Dynamics in Proteins: A Molecular Dynamics Simulation Analysis. *J. Phys. Chem. B* **2007,** *111*, 1482-1490.
17. Abbyad, P.; Shi, X.; Childs, W.; McAnaney, T. B.; Cohen, B. E.; Boxer, S. G., Measurement of Solvation Responses at Multiple Sites in a Globular Protein. *J. Phys. Chem. B* **2007,** *111*, 8269-8276.
18. Zhang, L.; Wang, L.; Kao, Y.-T.; Qiu, W.; Yang, Y.; Okobiah, O.; Zhong, D., Mapping Hydration Dynamics Around a Protein Surface. *Proc. Natl. Acad. Sci. USA* **2007,** *104*, 18461-18466.
19. Li, T.; Hassanali, A. A.; Kao, Y.-T.; Zhong, D.; Singer, S. J., Hydration Dynamics and Time Scales of Coupled Water-Protein Fluctuations. *J. Am. Chem. Soc.* **2007,** *129*, 3376-3382.

20. Posey, L. A.; Hendricks, R. J.; Beck, W. F., Dynamic Stokes Shift of the Time-Resolved Phosphorescence Spectrum of Zn^{II}-Substituted Cytochrome *c*. *J. Phys. Chem. B* **2013,** *117*, 15926−15934.
21. Kuo, Y.-H.; Chiang, Y.-W., Slow Dynamics around a Protein and Its Coupling to Solvent. *ACS Cent. Sci.* **2018,** *4*, 645−655.
22. Zhuravleva, A. V.; Korzhnev, D. M.; Kupce, E.; Arseniev, A. S.; Billeter, M.; Orekhov, V. Y., Gated Electron Transfers and Electron Pathways in Azurin: A NMR Dynamic Study at Multiple Fields and Temperatures. *J. Mol. Biol.* **2004,** *342*, 1599–1611.
23. Kalverda, A. P.; Ubbink, M.; Gilardi, G.; Wijmenga, S. S.; Crawford, A.; Jeuken, L. J. C.; Canters, G. W., Backbone Dynamics of Azurin in Solution: Slow Conformational Change Associated with Deprotonation of Histidine 35. *Biochemistry* **1999,** *38*, 12690-12697.
24. Korzhnev, D. M.; Karlsson, B. G.; Orekhov, V. Y.; Billeter, M., NMR Detection of Multiple Transitions to Low-Populated States in Azurin. *Protein Science* **2003,** *12*, 56–65.
25. Blanco-Rodríguez, A. M.; Busby, M.; Ronayne, K. L.; Towrie, M.; Grădinaru, C.; Sudhamsu, J.; Sýkora, J.; Hof, M.; Záliš, S.; Di Bilio, A. J.; Crane, B. R.; Gray, H. B.; Vlček, A., Jr., Relaxation Dynamics of $[Re^{I}(CO)_3(phen)(HisX)]^+$ (X = 83, 107, 109, 124, 126) *Pseudomonas aeruginosa* Azurins. *J. Am. Chem. Soc.* **2009,** *131*, 11788-11800.
26. Amaro, M.; Brezovsky, J.; Kováčová, S.; Sýkora, J.; Bednář, D.; Němec, V.; Lišková, V.; Kurumbang, N. G.; Beerens, K.; Chaloupková, R.; Paruch, K.; Hof, M.; Damborský, J., Site-Specific Analysis of Protein Hydration Based on Unnatural Amino Acid Fluorescence. *J. Am. Chem. Soc.* **2015,** *137*, 4988−4992.
27. Cohen, B. E.; McAnaney, T. B.; Park, E. S.; Jan, Y. N.; Boxer, S. G.; Jan, L. Y., Probing Protein Electrostatics with a Synthetic Fluorescent Amino Acid. *Science* **2002,** *296*, 1700-1703.
28. Zang, C.; Stevens, J. A.; Link, J. J.; Guo, L.; Wang, L.; Zhong, D., Ultrafast Proteinquake Dynamics in Cytochrome *c*. *J. Am. Chem. Soc.* **2009,** *131*, 2846-2852.
29. Sýkora, J.; Brezovský, J.; Koudeláková, T.; Lahoda, M.; Fořtová, A.; Chernovets, T.; Chaloupková, R.; Štěpánková, V.; Prokop, Z.; Smatanová, I. K.; Hof, M.; Damborský, J., Dynamics and Hydration Explain Failed Functional Transformation in Dehalogenase Design. *Nat. Chem. Biol.* **2014,** *10*, 428-430.
30. Jesenská, A.; Sýkora, J.; Olzynska, A.; Brezovský, J.; Zdráhal, Z.; Damborský, J.; Hof, M., Nanosecond Time-Dependent Stokes Shift at the Tunnel Mouth of Haloalkane Dehalogenases. *J. Am. Chem. Soc.* **2009,** *131*, 494–501.
31. Guha, S.; Sahu, K.; Roy, D.; Mondal, S. K.; Roy, S.; Bhattacharyya, K., Slow Solvation Dynamics at the Active Site of an Enzyme: Implications for Catalysis. *Biochemistry* **2005,** *44*, 8940-8947.
32. Horng, M. L.; Gardecki, J. A.; Papazyan, A.; Maroncelli, M., Subpicosecond Measurements of Polar Solvation Dynamics: Coumarin 153 Revisited. *J. Phys. Chem.* **1995,** *99*, 17311-17337.
33. Richert, R.; Stickel, F.; Fee, R. S.; Maroncelli, M., Solvation Dynamics and the Dielectric Response in a Glass-Forming Solvent: From Picoseconds to Seconds. *Chem. Phys. Lett.* **1994,** *229*, 302-308.
34. Glasbeek, M.; Zhang, H., Femtosecond Studies of Solvation and Intramolecular Configurational Dynamics of Fluorophores in Liquid Solution. *Chem. Rev.* **2004,** *104*, 1929-1954.
35. Halder, M.; Mukherjee, P.; Bose, S.; Hargrove, M. S.; Song, X.; Petrich, J. W., Solvation Dynamics in Protein Environments: Comparison of Fluorescence Upconversion Measurements of Coumarin 153 in Monomeric Hemeproteins with Molecular Dynamics Simulations. *J. Chem. Phys.* **2007,** *127*, 055101/055101-055101/055106.
36. Pal, S. K.; Zewail, A. H., Dynamics of Water in Biological Recognition. *Chem. Rev.* **2004,** *104*, 2099-2123.
37. Blanco-Rodríguez, A. M.; Busby, M.; Grădinaru, C.; Crane, B. R.; Di Bilio, A. J.; Matousek, P.; Towrie, M.; Leigh, B. S.; Richards, J. H.; Vlček, A., Jr.; Gray, H. B., Excited-State Dynamics of Structurally Characterized $[Re^{I}(CO)_3(phen)(HisX)]^+$ (X = 83, 109) Pseudomonas aeruginosa Azurins in Aqueous Solution. *J. Am. Chem. Soc.* **2006,** *128*, 4365-4370.

38. Blanco-Rodríguez, A. M.; Ronayne, K. L.; Záliš, S.; Sýkora, J.; Hof, M.; Vlček, A., Jr., Solvation-Driven Excited-State Dynamics of [Re(4-Et-pyridine)$(CO)_3$(2,2'-bipyridine)]$^+$ in Imidazolium Ionic Liquids. A Time-Resolved Infrared and Phosphorescence Study. *J. Phys. Chem. A* **2008,** *112*, 3506-3514.
39. Asbury, J. B.; Wang, Y.; Lian, T., Time-Dependent Vibration Stokes Shift During Solvation: Experiment and Theory. *Bull. Chem. Soc. Jpn.* **2002,** *75*, 973-983.
40. Liard, D. J.; Busby, M.; Matousek, P.; Towrie, M.; Vlček, A., Jr., Picosecond Relaxation of ^{3}MLCT Excited States of [Re(Etpy)$(CO)_3$(dmb)]$^+$ and [Re(Cl)$(CO)_3$(bpy)] as Revealed by Time-Resolved Resonance Raman, IR and UV-Vis Absorption Spectroscopy. *J. Phys. Chem. A* **2004,** *108*, 2363-2369.
41. Wang, H.; Lin, S.; Allen, J. P.; Williams, J. C.; Blankert, S.; Laser, C.; Woodbury, N. W., Protein Dynamics Control the Kinetics of Initial Electron Transfer in Photosynthesis. *Science* **2007,** *316*, 747-750.
42. Kundu, M.; He, T.-F.; Lu, Y.; Wang, L.; Zhong, D., Short-Range Electron Transfer in Reduced Flavodoxin: Ultrafast Nonequilibrium Dynamics Coupled with Protein Fluctuations. *J. Phys. Chem. Lett.* **2018,** *9*, 2782−2790.
43. Lu, Y.; Zhong, D., Understanding Short-Range Electron-Transfer Dynamics in Proteins. *J. Phys. Chem. Lett.* **2019,** *10*, 346−351.
44. Sumi, H.; Marcus, R. A., Dynamical effects in electron transfer reactions. *J. Chem. Phys.* **1986,** *84*, 4894-4914.
45. El Nahhas, A.; Consani, C.; Blanco-Rodríguez, A. M.; Lancaster, K. M.; Braem, O.; Cannizzo, A.; Towrie, M.; Clark, I. P.; Záliš, S.; Chergui, M.; Vlček, A., Jr., Ultrafast Excited-State Dynamics of Rhenium(I) Photosensitizers [Re(Cl)$(CO)_3$(N,N)] and [Re(imidazole)$(CO)_3$(N,N)]$^+$: Diimine Effects. *Inorg. Chem.* **2011,** *50*, 2932–2943.
46. Fumanal, M.; Daniel, C., Electronic and Photophysical Properties of [Re(L)$(CO)_3$(phen)]$^+$ and [Ru$(L)_2(bpy)_2]^{2+}$ (L = imidazole), Building Units for Long-Range Electron Transfer in Modified Blue Copper Proteins. *J. Phys. Chem. A* **2016,** *120*, 6934−6943.
47. Mai, S.; González, L., Unconventional Two-Step Spin Relaxation Dynamics of [Re$(CO)_3$(im)(phen)]$^+$ in Aqueous Solution. *Chem. Sci.* **2019,** *10*, 10405–10411.
48. Mai, S.; Gattuso, H.; Fumanal, M.; Muñoz-Losa, A.; Monari, A.; Daniel, C.; González, L.; Webb, S. E. D., Excited States of a Rhenium Carbonyl Diimine Complex: Solvation Models, Spin–Orbit Coupling, and Vibrational Sampling Effects. *Phys. Chem. Chem. Phys.* **2017,** *19*, 27240-27250.
49. Baková, R.; Chergui, M.; Daniel, C.; Vlček, A., Jr.; Záliš, S., Relativistic Effects in Spectroscopy and Photophysics of Heavy-Metal Complexes Illustrated by Spin-Orbit Calculations of [Re(imidazole)$(CO)_3$(phen)]$^+$. *Coord. Chem. Rev.* **2011,** *255*, 975-989.
50. Vlček, A., Jr., Ultrafast Excited-State Processes in Re(I) Carbonyl-Diimine Complexes: From Excitation to Photochemistry. *Top. Organomet. Chem.* **2010,** *29*, 73-114.
51. Kiefer, L. M.; King, J. T.; Kubarych, K. J., Equilibrium Excited State Dynamics of a Photo-Activated Catalyst Measured with Ultrafast Transient 2DIR. *J. Phys. Chem. A* **2014,** *118*, 9853−9860.
52. Kiefer, L. M.; King, J. T.; Kubarych, K. J., Dynamics of Rhenium Photocatalysts Revealed through Ultrafast Multidimensional Spectroscopy. *Acc. Chem. Res.* **2015,** *48*, 1123−1130.
53. Sokolová, L.; Williamson, H.; Sýkora, J.; Hof, M.; Gray, H. B.; Brutschy, B.; Vlček, A., Jr. , Mass Spectrometric Characterization of Oligomers in *Pseudomonas aeruginosa* Azurin Solutions. *J. Phys. Chem. B* **2011,** *115*, 4790–4800.
54. Connick, W. B.; Di Bilio, A. J.; Hill, M. G.; Winkler, J. R.; Gray, H. B., Tricarbonyl(1,10-phenanthroline)(imidazole)rhenium(I): A Powerful Photooxidant for Investigations of Electron Tunneling in Proteins. *Inorg. Chim. Acta* **1995,** *240*, 169-173.
55. Di Bilio, A. J.; Crane, B. R.; Wehbi, W. A.; Kiser, C. N.; Abu-Omar, M. M.; Carlos, R. M.; Richards, J. H.; Winkler, J. R.; Gray, H. B., Properties of Photogenerated Tryptophan and Tyrosyl Radicals in Structurally Characterized Proteins Containing Rhenium(I) Tricarbonyl Diimines. *J. Am. Chem. Soc.* **2001,** *123*, 3181-3182.

56. Maroncelli, M.; Fee, R. S.; Chapman, C. F.; Fleming, G. R., Comment on "Dynamic Stokes Shifl in Coumarin: Is It Only Relaxation?". *J. Phys. Chem.* **1991,** *95*, 1012-1014.
57. Tobin, P. H.; Wilson, C. J., Examining Photoinduced Energy Transfer in *Pseudomonas aeruginosa* Azurin. *J. Am. Chem. Soc.* **2014,** *136*, 1793−1802.
58. Jurkiewicz, P.; Sýkora; Agnieszka Olžyńska; Humpolíčková, J.; Hof, M., Solvent Relaxation in Phospholipid Bilayers: Principles and Recent Applications. *J. Fluorescence* **2005,** *15*, 883-894.
59. Pal, S. K.; Mandal, D.; Sukul, D.; Sen, S.; Bhattacharyya, K., Solvation Dynamics of DCM in Human Serum Albumin. *J. Phys. Chem. B* **2001,** *105*, 1438-1441.
60. Humbs, W.; van Veldhoven, E.; Zhang, H.; Glasbeek, M., Sub-picosecond fluorescence dynamics of organic light-emitting diode *tris*(8-hydroxyquinoline) metal complexes. *Chem. Phys. Lett.* **1999,** *304*, 10–18.
61. Cannizzo, A.; Blanco-Rodríguez, A. M.; Nahhas, A.; Šebera, J.; Záliš, S.; Vlček, A., Jr.; Chergui, M., Femtosecond Fluorescence and Intersystem Crossing in Rhenium(I) Carbonyl-Bipyridine Complexes *J. Am. Chem. Soc.* **2008,** *130*, 8967-8974.
62. El Nahhas, A.; Cannizzo, A.; van Mourik, F.; Blanco-Rodríguez, A. M.; Záliš, S.; Vlček, A., Jr.; Chergui, M., Ultrafast Excited-State Dynamics of $[Re(L)(CO)_3(bpy)]^n$ Complexes: Involvement of the solvent *J. Phys. Chem. A* **2010,** *114*, 6361-6369.
63. Kumar, A.; Sun, S.-S.; Lees, A. J., Photophysics and Photochemistry of Organometallic Rhenium Diimine Complexes. *Top. Organomet. Chem.* **2010,** *29*, 1-35.
64. Kiefer, L. M.; Kubarych, K. J., Solvent Exchange in Preformed Photocatalyst-Donor Precursor Complexes Determines Efficiency. *Chem. Sci.* **2018,** *9*, 1527-1533.

TOC graphic